PCCP

Accepted Manuscript




ROYAL SOCIETY OF CHEMISTRY

www.rsc.org/pccp

Journal Name

RSCPublishing

ARTICLE

# How ABA Block Polymer Activate Cytochrome C in Toluene: Molecular Dynamics Simulation and Experimental Observation

Cite this: DOI: 10.1039/x0xx00000x

Gong Chen,[a] Xian Kong,[a] Jingying Zhu,[a] Diannan Lu*[a], Zheng Liu*[a]

Received ooth January 2012,
Accepted ooth January 2012

DOI: 10.1039/x0xx00000x

www.rsc.org/pccp

While conjugation of enzymes with ABA copolymer resulted in an increase of enzymatic activity in organic solvent, by several orders of magnitude, the underpinned mechanism is not fully uncovered, particularly at molecular level. In present work, a coarse-grained molecular dynamics simulation of Cytochrome C (Cyt c) conjugated with PEO-PPO-PEO block copolymers (ABA) in toluene was simulated with Cyt c as a control. It is shown that the hydrophilic segments (PEO) of conjugated block polymers tend to entangle around the hydrophilic patch of Cyt c, while hydrophobic segments (PPO) extend to toluene. At a lower temperature, the PEO tails tend to form the hairpin structure outside the conjugated protein, whereas the Cyt c-ABA conjugates tend to form larger aggregates. At a higher temperature, however, the PEO tails tend to adsorb onto the hydrophilic protein surface, thus improve the suspension of the Cyt c-ABA conjugates and, consequently, the contact with the substrate. Moreover, the temperature increases drive the conformational transition of the active site of Cyt c-ABA from "inactive state" to "activated state" and thus results in an enhanced activity. To validate above simulations, Cyt c was conjugated to F127, an extensively used ABA copolymer. By elevating temperature, a decrease in the average size of Cyt c-F127 conjugate while a great increase in the apparent activity in toluene was observed, as can be predicted from the molecular dynamic simulation. The above mentioned molecular simulations offer a molecular insight of the temperature responsive behaviour of protein-ABA copolymers, which is helpful for the design and application of enzyme-polymer conjugates for industrial biocatalysis.

## Introduction

Enhancing the stability and activity of enzyme, which, by nature, performs catalysis in aqueous media, in organic media would essentially enable an advancement in chemical synthesis in terms of high regio-, stereo-, enantio- and chemical selectivity and high yield at mild conditions. While the conventional enzyme immobilization method offers a way to operate enzymes, the apparent activity in apolar solvents such as chloroform, toluene and etc., is often reduced by 1 to 2 orders of magnitude. This is mainly due to the poor suspension of enzyme catalyst in those solvents, which hinders the uptake of enzyme substrate. To address these problems, various nanostructures have been introduced to fabricate nanostructured enzyme catalysts for chemical synthesis in organic media, such as substrate and PEG imprinted enzyme nanogel[1], encapsulation into interpenetrated polymer network[2]. More recently, Zhu et al[3] showed that, by conjugating to Pluronic®, an ABA copolymer that is widely used for drug delivery[4-6] and preparation of mesoporous materials[7, 8], the apparent activity of enzyme conjugate in toluene increased by 50- to 670- fold, as compared to their native counterparts. The recovery of the enzyme conjugate is easily accomplished by cooling down the reaction system below the UCST of the enzyme-Pluronic conjugate. The application potential of the conjugate was demonstrated by the synthesis of valrubicin using lipase-Pluronic conjugate in MIBK[9] and the asymmetrical ammonolysis of (R)- and (S)-phenylglycine methyl ester using a CALB (lipase)-Pluronic nanoconjugate in tertiary butanol[10].

While the temperature responsiveness of Pluronic polymer is addressed by molecular dynamics simulation[11], the molecular insight of the interaction between the enzyme and polymer and its impact on the temperature responsiveness of the conjugate and, more importantly, the enhanced catalytic performance of the conjugated enzyme is not fully uncovered. These two issues are of fundamental importance to both the fabrication and application of the enzyme-polymer conjugate.

In the present study, coarse-grained models of Cyt c-ABA conjugate and its native counterpart, Cyt c, were established. Molecular dynamics simulations were conducted to monitor the structure activation of the conjugated Cyt c and its active sites, temperature-induced self-assembly conformation transition of Cyt c-ABA conjugate and its impacts on stability and activity of Cyt c-ABA conjugate in toluene. The aggregation and suspension of Cyt c-ABA and Cyt c were probed from free energy and contact number analysis. Cyt c-F127 conjugate was synthesized and subjected to the solvation and catalysis at different temperatures in toluene. Based on above simulations and experiments, a comprehensive description on the temparture responsiveness of the Cyt c-ABA was established as molecular fundamentals for the design and application of enzyme-polymer conjugates for chemical synthesis in organic media.

## Materials and methods

### Model

The native structure of *Cytochrome C* was obtained from the Protein Data Bank (PDB code: 1AKK[12]). Coarse-grained models of both Cyt c-ABA and Cyt c with Martini force field were established according to Marinize method[13, 14] as shown in Figure 1. In brief, all coarse-grained beads of both Cyt c and PEO-PPO-PEO(Pluronic) have a mass of 72 amu, while ring bead for toluene (SC5) has a mass of 45 amu. The total charge of Cyt c is -9.0. The amino acids of Cyt c, who covalently or non-covalently bond to HEME C, are defined as the active site of Cyt c.

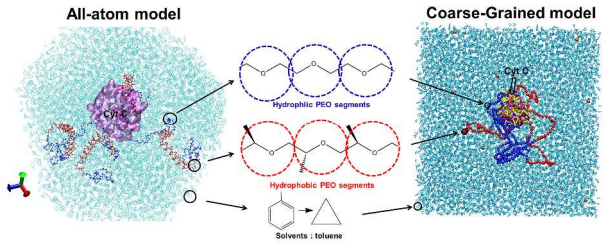


**Fig.1** Molecular model for Cyt c-ABA conjugate

Here we choose Pluronic P85, which consists of 40 hydrophobic PPO units in the middle of polymer and 26 hydrophilic PEO units on each end of polymer to form ABA type block polymer. The atomic groups of C-C-O and C($CH_3$)-C-O are considered as coarse-grained beads of PEO and PPO segments, respectively as shown in Fig. 1. The molecular simulation of PEO-PPO-PEO has been reported in the cases of its interaction with lipids[15-17], its function as pharmaceutical molecules[18], and the micelle structure in aqueous solution[19]. Here the parameters of PEO and PPO, are obtained from Samira Hezaveh[17] in Martini force field based on their atomistic model. For Cyt c-ABA conjugate, four Pluronic P85 chains were covalently attached on the $Lys^{22}$, $Lys^{53}$, $Lys^{73}$ and $Lys^{99}$ of Cyt c with distance of 3.8 Å between side chain bead SC2 of lysine and first bead of P85. The reason of choosing these four lysines is that the pKa values of these lysines in Cyt c, as calculated by H++ tool[20] (http://biophysics.cs.vt.edu/), is higher than 7.0 and thus facilitates the formation of covalent bond between aldehyde P85 and Cyt c. A model of Cyt c and Pluronic F127, which has more PEO and PPO units, was also built for the ease of direct comparison with experimental results. The details were given in SI. (Fig. S8)

The organic solvent, toluene, was described by the three-beads model proposed by de Jong et al[21].

### Simulation and Analytical Method

All MD simulations were conducted with the MD software Gromacs 4.5.4-5.0.0[22]. The V-rescale[23] and Berendsen methods[24] were used to maintain temperature and pressure (1 bar) to the reference values with coupling time constant of 0.5 ps and 3.0 ps, respectively. The Lennard-Jones and electrostatic interactions were smoothly shifted from 0.9 nm to 1.2 nm and 0.0 nm to 1.2 nm, respectively. The integration time step was 20 fs. During the simulations, Cyt c-ABA conjugates were placed in the centre of rectangular box using the periodic boundary conditions. Firstly, the energy minimization was performed to minimize the energy of conjugates in vacuum to 200 $kJ \cdot mol^{-1} \cdot nm^{-1}$. Then restricted MD with fixed position of Cyt c was performed to allow the conjugated polymer chains to collapse to an appropriate size in vacuum. After these steps, toluene molecules were added into simulation box as solvents, and then energy minimization and restricted MD with fixed position of Cyt c were repeated to equilibrate solvents and ABA chains. For the product MD simulation at a given temperature, the starting conformation was obtained from the last few frames of the same pre-equilibrium simulation. 2 μs product runs were performed at given temperature and the properties were averaged from the last 1 μs. The snapshots were drawn by VMD 1.9.1[25].

In order to get the initial conformation for the calculation of free energy along the reaction coordinate, we used steered molecular dynamics (SMD) simulation to pull the PEO tail towards protein (Case 1) and separate two binding protein (Case 2), respectively. For all the SMD simulations, a pulling rate of $2\times10^{-5}$ $nm \cdot ps^{-1}$ and harmonic force constant of 1000 $kJ \cdot mol^{-1} \cdot nm^2$ was adopted. An umbrella sampling methods was adopted to calculate the free energy profiles of PEO tails adsorb onto the protein surface (Case 1) and two binding conjugates separate from each other (Case 2) at different temperature respectively. Starting conformations for umbrella sampling were taken from the SMD trajectory. The window width of 0.1 nm was adopted to ensure the consecutiveness of the PMF profile. Each window of case 1 and case 2 was simulated for 50 ns, 90 ns respectively. The weighted histogram analysis method (WHAM)[26] was adopted for the calculation of the PMF profile.

To obtain the aggregate size of conjugates and free Cyt c, the criterion for calculating the size of aggregates is described in Eq(1).

$$State = \begin{cases} \text{"Aggregated"} \ d_{COM} \le 4.8\ nm,\ \Delta t \ge 0.4\ \text{ns} \\ \text{"Collision"} \ d_{COM} \le 4.8\ nm,\ \Delta t < 0.4\ \text{ns} \\ \text{"Separated"} \ d_{COM} > 4.8\ nm \end{cases} \quad (1)$$

Where $d_{com}$ is the distance between centre of mass (COM) of conjugates or Cyt cs, and $\Delta t$ is the persisting time of two conjugates or two Cyt cs attaching to each other. According the values of $d_{com}$ and $\Delta t$, the states of conjugates or Cyt cs can grouped into three "states": "Aggregated state", in which two conjugates or Cyt cs form stable aggregates with $d_{com} \le 4.8$ nm and $\Delta t \ge 0.4$ ns, "Collision state" in which two conjugates or Cyt cs form unstable aggregate with $d_{com} \le 4.8$ nm and $\Delta t < 0.4$ ns, and "Separated state" in which conjugates or Cyt cs are well dispersed in solution with $d_{com} > 4.8$ nm.

So the aggregate size is defined as the number of conjugates or Cyt cs in aggregates. Another important parameter is the contact number, i.e., the contact number between beads of different conjugated Cyt cs.

To further understand the aggregating behaviour of conjugates, the contact areas ($S_c$) of two Cyt c of aggregated conjugates were calculated using Eq(2):

$$S_C = \frac{1}{2}(SAS_A + SAS_B - SAS_{A+B}) \quad (2)$$

where $S_c$ is the contact area of the two conjugated Cyt c denoted by A and B, respectively. $SAS_A$ is the solvent accessible area of conjugated Cyt c A, assuming that only Cyt c A is in simulation box. Similarly, $SAS_B$ is the solvent accessible area of conjugated Cyt c B, assuming that only Cyt c B is in simulation box. $SAS_{A+B}$ is the solvent accessible area of Cyt c A and Cyt c B, assuming both of them are in simulation box. And the calculated contact area was divided into hydrophilic patch and hydrophobic patch according to hydrophilicity of surficial amino acids of contact area. Moreover, we define a parameter α , which refers to the selectivity of contact area. In toluene, the more hydrophilic contact area is, the closer conjugates contact, using Eq(3).

$$\alpha = \frac{S_C(hydrophilic)}{S_C(hydrophobic)} \quad (3)$$

## Experimental Section

To validate the simulation, we synthesized Pluonric F127 conjugated Cyt c, denoted as Cyt c-F127, and measured its temperature-responsiveness from both solubility and activity in toluene, using the native Cyt c as a control. Compared to P85, conjugate F127 to Cyt c has a higher yield. We also performed the molecular dynamics simulation of Cyt c-F127 and obtained results similar to that of Cyt c-P85, which was described in Supporting Information.

Cyt c-F127 conjugates were synthesized using the methods invented by our lab[3]. Afterwards, 0.002 mM Cyt c-F127 in toluene was adopted for dynamics light scattering (Malvern, NanoZZ90, ZEN3690). 1,2-diaminobenzene and tert-butylhydroperoxide are chosen to evaluate the catalytic activity of conjugated and free Cyt c in toluene, where 1,2-diaminobenzene is oxidized by tert-butylhydroperoxide[27]. A portion (10 ml) of 50 mM 1,2- diaminobenzene in anhydrous toluene is mixed with 1 mL 25%v/v tert-butylhydroperoxide in toluene. Then Cyt c-F127 or free Cyt c containing 0.5 mg protein was added with constant stirring rate (200 rpm) under different temperatures for 10 min. The specific activity ( $SA$) is calculated from Eq (4).

$$SA = \frac{A_{470nm} - A_{blank\_470nm}}{0.1m\Delta t}\ U/mg \quad (4)$$

where $A_{470nm}$ is the absorbance of reacted solvents at 470 nm, $A_{blank\ 470nm}$ is absorbance value without enzyme catalysts, $m$ is the mass of Cyt c and $\Delta t$ is the reaction time.

## Results and discussion:

### Improved stability of conjugated Cyt c and activation of its active sites by temperature

Figure 2 gives root mean square deviation (RMSD) of Cyt cs and their active site, solvent accessible surface(SAS) for active sites of Cyt c, as well as snapshots of both conjugates and free Cyt c.

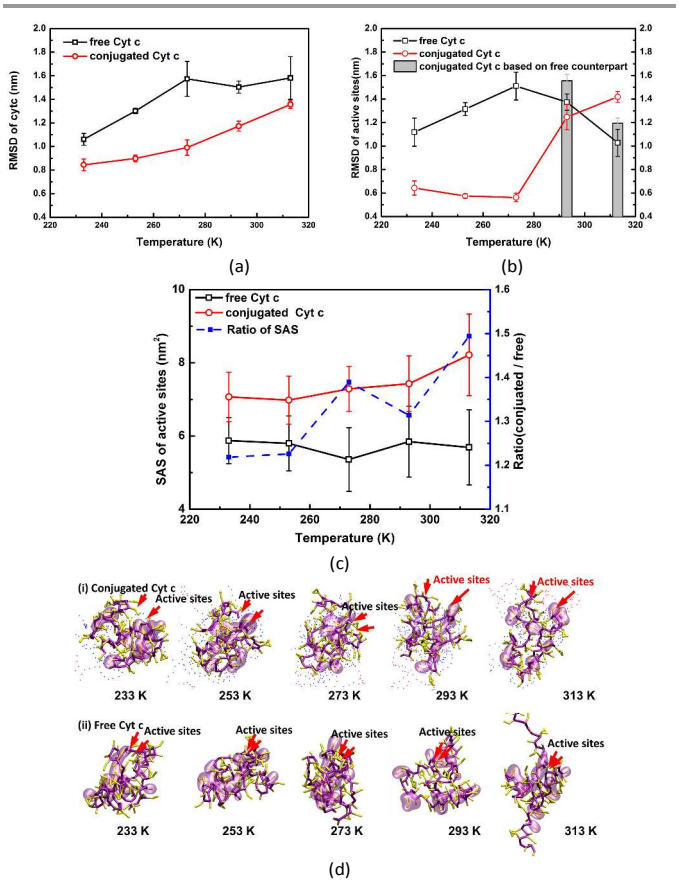


Fig. 2 (a) RMSD values of free Cyt c and conjugated Cyt c; (b) SAS of active sites of free and conjugated Cyt c as a function of temperature; (c) RMSD of active sites of free and conjugated Cyt c; (d) Snapshots for (i) conjugated Cyt c, (ii) free Cyt c

in toluene, backbone of Cyt c was rendered as purple licorice-bonds, yellow licorice-bonds for side chains of Cyt c, transparent surface for active sites, red points for PPO, blue points for PEO. For clarity, the pluronic chains are displayed as dots and solvents are not displayed. Red arrows show the entrance of the active pockets of Cyt c

As shown by Fig. 2(a), a less RMSD difference compared with the initial X-ray structure indicates that the conjugated Cyt c is more stable than the free Cyt c. This may attribute to the formation of PEO layer entangling around Cyt c (details in Fig. S1). While the hydrophobic interaction of PPO with toluene molecules leads to a greater radius of conjugated Cyt c than that of free Cyt c (details in Fig. S3). This benefits the access of substrates into the active centre.

Fig. 2(b) gives the RMSD of active site of conjugated Cyt c and native Cyt c at different temperatures. It is shown that when temperature is below 293 K, the active site of conjugated Cyt c has a negligible difference compared with the X-ray structure. When the temperature is above 293 K, however, the RMSD of the active sites of conjugated Cyt c undergoes a dramatic increase. And the difference in RMSD of the active site between conjugated Cyt c and its free counterpart at high temperature suggests that that the structure of active sites is distinct from the its free counterpart and the original x-ray structure. Fig. S4 gives the RMSF results of active sites of conjugated Cyt c and native Cyt c at different temperatures. It is shown that active sites of conjugated Cyt c undergoes less fluctuation, indicates active sites of conjugated Cyt c is more stable than its free counterpart.

The solvent accessible area of active site of conjugated Cyt c and its free counterpart are shown in Figure 2(c). It is shown that the conjugated Cyt c has a larger SAS than the free Cyt c and the ratio of conjugated Cyt c to free one raises from 1.2 to 1.5 when temperature increases from 233 K to 313 K. This suggests that the elevation of the conjugated Cyt c activity in response to temperature can be attributed to the increased accessible channels for substrates when temperature increases. Combining Fig. 2(b), Fig. S4 and Fig. 2(c), the active sites of conjugated Cyt c could be everted and keep stable, thus be more accessible to substrate in response to an environmental temperature rise, Here we named this eversion conformation as "activated states".

Fig. 2(d) gives the snapshots of the conjugated Cyt c and free Cyt c at different temperatures. It is shown that conjugated Cyt c maintains correct secondary structure when temperature rises from 233 K to 313 K. However, the backbone of the free Cyt c squeezes and unfolds at 313 K. This may attribute to the repulsive interaction between hydrophilic Cyt c and hydrophobic toluene molecules, which leads to the compact structure of free enzyme, despite that enzymes are usually more stable in anhydrous environment than in water. Compared with the free Cyt c, the conjugated Cyt c maintains the correctly folded conformation at the companion of Pluronic P85. More interestingly, the active site shown in transparent surface of conjugated Cyt c turns to be a more opened status at 293 K or higher temperatures, this facilitating the access of substrates(as shown in red arrow, Fig 2(d)).

**Pluronic chain Entangled around Cyt c in toluene at different temperatures**

We firstly simulated the self-assembled structure of conjugates to explore, firstly, how the structure of the conjugates affects the stability and activity; secondly, at what condition the conjugates assemble or disperse in a given solvent and, finally, how the conjugate responses to temperature.

As shown in Fig. 3(a), the inner PEO segments adsorb onto the surface of Cyt c while PPO segments expose to toluene, as we expected. The driving force for this assembly is hydrophilic interaction between PEO segments and surficial hydrophilic amino acids of Cyt c since PEO segments are relatively more hydrophilic than PPO segments[28]. On the other hand, the hydrophobic PPO segments prefers the weak-polar or apolar environment and thus extends in toluene.

As shown in Fig 3(a), PEO tails of conjugated Pluronic P85 tend to form the ordered hairpin structure at 233 K. At a higher temperature, PEO tails entangle onto the protein surface. The ordered parameter of PEO tails (as shown in Fig. S5) decreases remarkably when temperature increases from 233 K to 253 K, indicating the dissociation of the hairpin structure, which is important for the aggregating of conjugated Cyt c at low temperature. The detailed discussion will be given the following section.

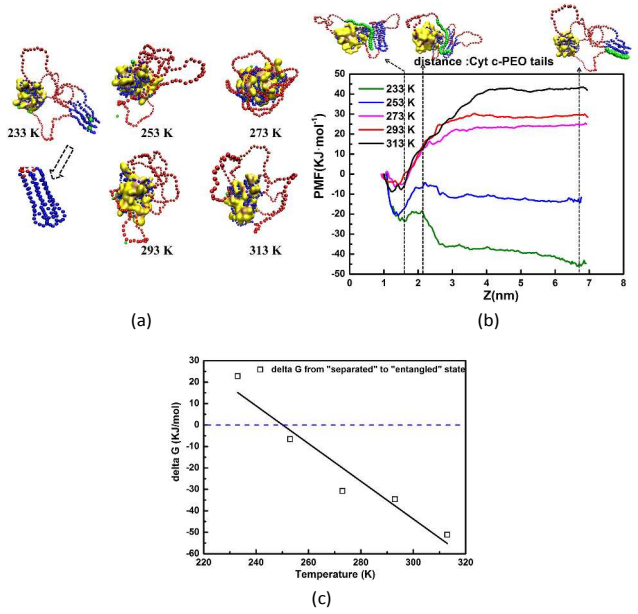


Fig. 3 (a) the geometry of the conjugates; (b)PMF curves of pulling PEO tails towards protein at different temperatures;(c) Relation between Gibbs free energy difference and temperature

The free energy changes of PEO tails to move from the distant position towards the protein surface under different temperatures were calculated using PMF method. As shown in Fig 3(b) and Fig 3(c), the energy barrier for PEO tails to move from the distant position towards the protein surface is almost linearly decreases as temperature increases as Eq(5) describes。

$$(\frac{\partial G}{\partial T})_p = -S \qquad (5)$$

It means PEO tails could move towards the surface of Cyt c spontaneously, when temperature is raised to 253 K or even higher. However PEO tails need to overcome the energy barrier of 22.77 KJ/mol to reach the surface of Cyt c at low temperature. These quantitative results agree with the different assemble structures of PEO tails under different temperatures. Moreover, these results illustrate that the temperature responsiveness is determined by free energy barrier for PEO tails from distant position to the surface of protein at low temperature. That is, the aggregating of PEO segment at low temperature is the driving force for precipitation of conjugated Cyt c.

**Aggregation of two Pluronic-conjugated Cyt c molecules**

The aggregation of Pluronic-conjugated enzyme at a lower temperature facilitates the recovery of the enzyme catalyst after the reaction. While the protein aggregation is extensively investigated, the aggregation of Pluronic-conjugated protein in organic solvents is, to our knowledge, not addressed by far. Here we started by simulating the aggregation of two Pluronic-conjugated Cyt c molecules in toluene. The yield of aggregate from 10 times randomly positioned simulation was 10% at 233 K and 0% at 313 K. And as shown in Fig. S6, the criterion for aggregation is 4.8 nm. That is, when COM is below 4.8 nm, the two conjugated Cyt c forms aggregate.

The aggregation behaviour of two conjugated Cyt cs were simulated by pulling them from the aggregated state to a separated state. Through analysis of pulling trajectory, results show that the PEO segments bridge the two conjugated Cyt cs during pulling process and get in the way of the dispersion of conjugates as shown in Fig 4.

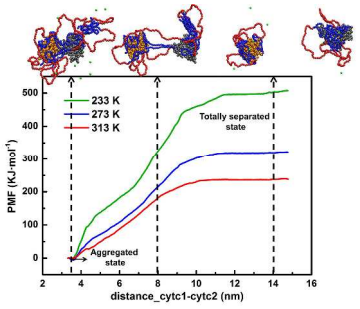


Fig. 4 PMF curves of pulling two conjugates separately at different temperatures

Next, free energy barriers were calculated along the reaction coordinate by above-mentioned PMF method. Free energy changes from aggregated state to totally separated state of two conjugates are defined as aggregation energy in our research. Thus, the PMF curves in Fig 4 show that the aggregation energy decreases from the highest 502.76 kJ/mol at 233 K to 321.20 kJ/mol at 273 K and finally reach the lowest 236.22 kJ/mol at 313 K, which account for only 47% of aggregation energy at 233 K.

It could be concluded that the free energy barrier from the aggregated state to separated state is higher at lower temperature, indicating that low temperature favours the aggregation of conjugated Cyt c. This may attribute to intensified hydrophilic interaction between protein surface and PEO segments, and meanwhile, weakened thermal motion.

**Aggregation of four conjugated Cyt c molecules**

We further simulated the aggregation of 4 Cyt c-Pluronic P85 conjugate biomolecules at 233 K and 313 K, respectively. The results are shown in Fig 5. We firstly analysed RMSD of each Cyt c at 233 K and 313 K as shown in Fig 5(a) and Fig. 5 (b). It is shown that RMSD of conjugated Cyt c turns to be flat during the initial 200 ns and keep constant, i.e., 6.6 Å on average at 233 K and 11.7 Å on average at 313 K, respectively. This is consistent with that determined in single conjugated Cyt c system, as shown in Fig 2(a). The average RMSDs of four free Cyt c are 11.9 Å and 14.9 Å at 233 K and 313 K, respectively, which are also the same as those determined in a single-Cyt c system. However, RMSD values of the single Cyt c fluctuate more intensely during the whole simulation, indicating that, compared to single-enzyme system, Pluronic-conjugated Cyt c is more stable.

The average contact number between amino acids of four Cyt c (criterion is 0.6 nm) was calculated and shown in Fig 5(c). It shows that contact number of conjugates is much smaller at high temperature, indicates the aggregation behaviour of conjugates is temperature responsive and the conjugates is dispersed better at high temperature. This agrees with temperature-responsive self-assembled conformations of single conjugate and temperature induced different free energy barriers to separate two binding conjugates, as described in Fig 4.

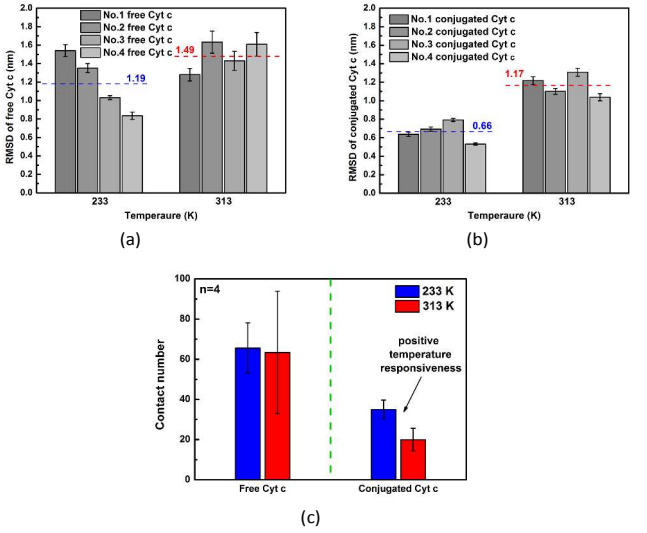


Fig. 5 Root mean square deviation (RMSD) values of (a)free Cyt c and (b) conjugated Cyt c; (c) Contact number for both conjugates and free Cyt c at different temperatures;

Based on Eq(1), the average aggregate size was calculated and shown in Fig. S7(a). And the same conclusion could be inferred that the aggregating behaviour of conjugates is temperature responsive and the conjugate is dispersed better at high temperature. The size of the free Cyt c is large than 2 at both a low and high temperature, indicating that the solubility of free Cyt c is poor in non-polar organic media, as experimentally observed elsewhere[29].

**Experimental validation**

Fig 6 shows the average size of F127-Cyt c determined by DLS as a function of temperature. Fig 6(a) shows that the average size of F127-Cyt c decreases from 1287 nm to 45.6 nm, almost linearly when temperature increases from 273 K to 313 K, which agrees well with the simulation results shown in Fig.4 and 5.

Fig 6(b) displays the activity of both free and conjugated Cyt c in toluene. It is shown that the optimal temperature for enzymatic catalyst is 293 K, a reduction of apparent activity when temperature is above 293 K is observed for both free and conjugated Cyt c, this may be attributed to the thermal deactivation[30]. Notably, a sharp increase in the activity ratio of Pluronic F127 conjugated Cyt c to free one from 4.0 to 7.5 is obtained when temperature increases from 303 to 313 K. This, we believe, can be attributed to, firstly, an improved dispersion of the conjugate, as experimentally observed (Fig. 6(a)) and simulation (Fig. 4 and 5.), and secondly, the activation effects(Fig. 2).

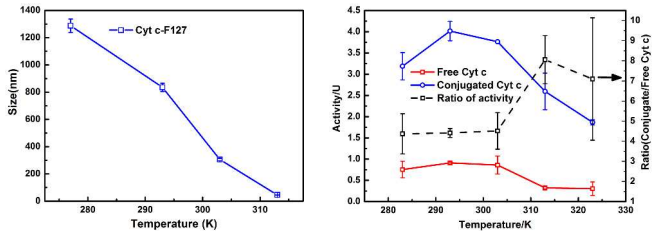


Fig. 6 (a)Average size of Cyt c- F127 conjugates detected by DLS as a function of temperature(b) Specific Activity of free and F127 conjugated Cyt c as a function of temperature

## Conclusions

The present study has shown, by molecular dynamics simulation, that Pluronic P85 conjugated Cyt c is more stable than free Cyt c in toluene, in which PEO segments tend to entangle around hydrophilic surface of Cyt c while PPO segments extend to toluene. The increase in temperature from 273 K to 313 K led to an transition of the active sites of conjugated Cyt c from "inactive state" to "activated state", which is more accessible to substrate. The free Cyt c does not show such phenomena. It is also shown that, at a low temperature, PEO tails tend to form the ordered hairpin structure away from Cyt c and thus favours the formation of large aggregates. This thus hindered the access of substrate to the active sites of the conjugated Cyt c but facilitated the recovery of conjugates after the reaction. At a high temperature, PEO tails tend to entangle onto the protein surface driving by hydrophilic interactions and thus facilitated the dispersion of conjugates and the access of substrates to the active site. The experiments confirm an improved dispersion of Cyt c-Pluronic F127 conjugates in toluene, and simultaneously, greatly enhanced activity, in response to temperature increases, as predicted by molecular simulation. The present work offered a molecular insight of the temperature responsiveness of protein-ABA copolymer, as represented by Cyt c-Pluronic, which can be applied for the design and application of enzyme-polymer conjugates.

## Acknowledgements

The authors are grateful to the Chinese National Natural Science Foundation for financial support of this project (No. 21036003 and 21276138) and Tsinghua University Foundation (No. 2013108930).

## Notes and references

[a] Department of Chemical Engineering, Tsinghua University, Beijing, 100084, China.
E-mail: ludiannan@tsinghua.edu.cn, liuzheng@mail.tsinghua.edu.cn

Electronic Supplementary Information (ESI) available: [details of any supplementary information available should be included here]. See DOI: 10.1039/b000000x/

1. R. Wang, Y. Zhang, J. Huang, D. Lu, J. Ge and Z. Liu, *Green Chemistry*, 2013, **15**, 1155-1158.
2. M. Du, D. Lu and Z. Liu, *Journal of Molecular Catalysis B: Enzymatic*, 2013, **88**, 60-68.
3. J. Zhu, Y. Zhang, D. Lu, R. N. Zare, J. Ge and Z. Liu, *Chem. Commun.*, 2013.
4. N. Wang, Y. P. Guan, L. R. Yang, L. W. Jia, X. T. Wei, H. Z. Liu and C. Guo, *J Colloid Interf Sci*, 2013, **395**, 50-57.
5. T. K. Jain, M. A. Morales, S. K. Sahoo, D. L. Leslie-Pelecky and V. Labhasetwar, *Molecular Pharmaceutics*, 2005, **2**, 194-205.
6. P. Lemieux, N. Guerin, G. Paradis, R. Proulx, L. Chistyakova, A. Kabanov and V. Alakhov, *Gene therapy*, 2000, **7**, 986-991.
7. F. Li, M. B. Wilker and A. Stein, *Langmuir*, 2012, **28**, 7484-7491.
8. T. W. Kim, F. Kleitz, B. Paul and R. Ryoo, *Journal of the American Chemical Society*, 2005, **127**, 7601-7610.
9. Y. Zhang, Y. Dai, M. Hou, T. Li, J. Ge and Z. Liu, *RSC Advances*, 2013, **3**, 22963-22966.
10. X. Wu, R. Wang, Y. Zhang, J. Ge and Z. Liu, *Catalysis Letters*, 2014, **144**, 1407-1410.
11. G. Chen, J. Zhu, J. Ge, D. Lu and Z. Liu, *CIESC Journal*, 2014, **65**, 4157-4167.
12. L. Banci, I. Bertini, H. B. Gray, C. Luchinat, T. Reddig, A. Rosato and P. Turano, *Biochemistry*, 1997, **36**, 9867-9877.
13. S. J. Marrink, H. J. Risselada, S. Yefimov, D. P. Tieleman and A. H. de Vries, *The Journal of Physical Chemistry B*, 2007, **111**, 7812-7824.

14. L. Monticelli, S. K. Kandasamy, X. Periole, R. G. Larson, D. P. Tieleman and S.-J. Marrink, *Journal of Chemical Theory and Computation*, 2008, **4**, 819-834.
15. S. Samanta, S. Hezaveh and D. Roccatano, *The Journal of Physical Chemistry B*, 2013.
16. S. Nawaz, M. Redhead, G. Mantovani, C. Alexander, C. Bosquillon and P. Carbone, *Soft Matter*, 2012, **8**, 6744-6754.
17. S. Hezaveh, S. Samanta, A. De Nicola, G. Milano and D. Roccatano, *Journal of Physical Chemistry B*, 2012, **116**, 14333-14345.
18. S. Samanta and D. Roccatano, *The Journal of Physical Chemistry B*, 2013, **117**, 3250-3257.
19. D. Bedrov, C. Ayyagari and G. D. Smith, *Journal of Chemical Theory and Computation*, 2006, **2**, 598-606.
20. J. C. Gordon, J. B. Myers, T. Folta, V. Shoja, L. S. Heath and A. Onufriev, *Nucleic acids research*, 2005, **33**, W368-W371.
21. D. H. de Jong, G. Singh, W. D. Bennett, C. Arnarez, T. A. Wassenaar, L. V. Schafer, X. Periole, D. P. Tieleman and S. J. Marrink, *Journal of Chemical Theory and Computation*, 2012, **9**, 687-697.
22. S. Pronk, S. Páll, R. Schulz, P. Larsson, P. Bjelkmar, R. Apostolov, M. R. Shirts, J. C. Smith, P. M. Kasson and D. van der Spoel, *Bioinformatics*, 2013, btt055.
23. G. Bussi, D. Donadio and M. Parrinello, *The Journal of chemical physics*, 2007, **126**, 014101.
24. H. J. Berendsen, J. P. M. Postma, W. F. van Gunsteren, A. DiNola and J. Haak, *The Journal of chemical physics*, 1984, **81**, 3684-3690.
25. W. Humphrey, A. Dalke and K. Schulten, *Journal of molecular graphics*, 1996, **14**, 33-38.
26. S. Kumar, J. M. Rosenberg, D. Bouzida, R. H. Swendsen and P. A. Kollman, *Journal of computational chemistry*, 1992, **13**, 1011-1021.
27. H. Takahashi, B. Li, T. Sasaki, C. Miyazaki, T. Kajino and S. Inagaki, *Chemistry of Materials*, 2000, **12**, 3301-3305.
28. R. Ganguly, V. Aswal, P. Hassan, I. Gopalakrishnan and S. Kulshreshtha, *The Journal of Physical Chemistry B*, 2006, **110**, 9843-9849.
29. E. Escamilla, G. Ayala, M. T. de Gómez-Puyou, A. Gómez-Puyou, L. Millán and A. Darszon, *Archives of biochemistry and biophysics*, 1989, **272**, 332-343.
30. H. García-Arellano, B. Valderrama, G. Saab-Rincón and R. Vazquez-Duhalt, *Bioconjugate chemistry*, 2002, **13**, 1336-1344.